Synaptotagmin SYTA forms ER-plasma membrane junctions that are recruited to plasmodesmata for plant virus movement

Amit Levy, **Judy Y. Zheng**, and **Sondra G. Lazarowitz**[1]

Department of Plant Pathology and Plant-Microbe Biology, Cornell University, Ithaca, NY 14853, USA

Keywords

Summary

Metazoan synaptotagmins are Ca^{2+} sensors that regulate exocytosis and endocytosis in various cell types, notably nerve and neuroendocrine cells [1, 2]. Recently, the structurally related extended synaptotagmins were shown to tether the cortical ER to the plasma membrane in human and yeast cells to maintain ER morphology and stabilize ER-plasma membrane (ER-PM) contact sites for intracellular lipid and Ca^{2+} signaling [3, 4]. The Arabidopsis synaptotagmin SYTA regulates endocytosis and the ability of plant virus movement proteins (MPs) to alter plasmodesmata to promote virus cell-to-cell transport [5, 6]. Yet, how MPs modify plasmodesmata, the cellular functions of SYTA and how these aid MP activity, and the proteins essential to form plant cell ER-PM contact sites remain unknown. We addressed these questions using an Arabidopsis SYTA knockdown line *syta-1* and a Tobamovirus movement protein MP^{TVCV} [5, 7]. We report here that SYTA localized to ER-PM contact sites. These sites were depleted and the ER network collapsed in *syta-1*, and both reformed upon rescue with SYTA. MP^{TVCV} accumulation in plasmodesmata, but not secretory trafficking, was also inhibited in *syta-1*. During infection, MP^{TVCV} recruited SYTA to plasmodesmata, and SYTA and the cortical ER were subsequently remodeled to form viral replication sites adjacent to plasmodesmata in which MP^{TVCV} and SYTA directly interacted caged within ER membrane. SYTA also accumulated in plasmodesmata active in MP^{TVCV} transport. Our findings show that SYTA is essential to form ER-PM contact sites and suggest that MPs interact with SYTA to recruit these sites to alter plasmodesmata for virus cell-to-cell movement.

[1]Corresponding author: SGL5@cornell.edu, phone: (607) 255-7830, (607) 229-3059, FAX: (607) 255-4471.

Results and Discussion

Movement proteins (MPs) mediate cell-to-cell transport of viral genomes across the plant cell wall for local and systemic infection. Different models for how diverse plant viruses accomplish this share three key features: MPs alter the permeability of plasmodesmata (PD), complex trans-wall channels that regulate plant cell-cell communication; MPs coordinate the replication of viral genomes with their transport to PD; and the ER and vesicle transport are required for distinct MPs to traffic to and alter PD [6, 8]. Despite intense efforts, we do not understand how selective transport occurs through PD, nor how viral MPs reach PD and alter their permeability. Arabidopsis SYNAPTOTAGMIN A (*At*SYTA, a.k.a. *At*SYT1; hereafter SYTA) regulates MP-mediated cell-to-cell movement for diverse plant viruses [5, 6]. SYTA is one of five synaptotagmins (SYTs) encoded by *Arabidopsis thaliana* [5, 9], all of which are predicted to have the domain structure that typifies their animal orthologs: an uncleaved signal peptide and overlapping N-terminal transmembrane domain, followed by a cytosolic variable region and tandem C2 Ca^{2+}/lipid-binding domains, C2A and C2B [1, 2]. SYTs are evolutionarily conserved in metazoans and plants, but not found in yeast [9]. Mammalian SYT1, the best studied SYT, acts as a Ca^{2+} sensor to trigger rapid exocytosis of neurotransmitters or hormones in neurons or neuroendocrine cells, and to regulate endocytosis to retrieve cell surface membrane [1, 2]. Key to these activities are C2A and C2B, which, upon binding Ca^{2+}, interact with cellular proteins and plasma membrane lipids to mediate membrane fusion for exocytosis or regulate endocytosis [1, 10–12]. Metazoan SYTs comprise a large gene family, and they vary widely in their affinity for Ca^{2+} and regulate exo/endocytosis in a variety of cell types [1, 2].

SYTA localizes to ER-PM contact sites

Mammals encode three SYT-related extended synaptotagmins (E-SYT1, E-SYT2, and E-SYT3), which have three or five C2 domains. E-SYTs are ubiquitously expressed and evolutionarily conserved, including three orthologs in yeast (tricalbins Tcb1p, Tcb2p and Tcb3p), each with three C2 domains [4, 9, 13]. A second distinct feature from classical SYTs is an SMP domain within the E-SYT variable region [3, 4, 14]. These lipid-binding modules are proposed to function in lipid transfer at anchored zones between organelles called membrane contact sites [14]. Human E-SYTs and yeast Tcbs are ER-anchored proteins that tether the cortical ER to the plasma membrane via their C2 domains to maintain ER reticulate structure and stabilize ER-plasma membrane (ER-PM) contact sites for non-vesicular intracellular signaling. Like classical SYTs, SYTA has two C2 domains, regulates endocytosis in plant cells, and can be found on cytosolic vesicles. SYTA C2B is also essential to regulate endocytosis and MP-directed cell-to-cell transport via PD for diverse plant viruses, including the Tobamoviruses *Tobacco mosaic virus* (TMV) and *Turnip vein clearing virus* (TVCV) [5, 6]. But, similar to E-SYTs, SYTA localizes to discrete focal areas along the plasma membrane in plant cells [5, 15], and our analyses predicted an SMP domain between amino acid residues 69–248 in the SYTA variable domain and at the equivalent position in Arabidopsis SYTs B, C, D and E (Figures S1A and S1D). The SMP domain of human E-SYT2 forms a β-barrel that dimerizes to create a hydrophobic cylindrical channel, which can contain lipids [16]. Our modeling to this structure predicted that the SYTA SMP domain can form this characteristic β-barrel comprising a twisted β-

sheet and two α-helices, with a third helix partially capping one end of the barrel (Figures S1B–S1C).

To determine whether the focal areas of SYTA at the plasma membrane were ER-PM contact sites, we transiently co-expressed a functional SYTA-GFP fusion and the ER marker RFP-HDEL in *Nicotiana benthamiana* leaves [5, 17]. We also co-expressed SYTA-RFP and Arabidopsis VAP27-GFP. VAP27, a plant homolog of the yeast ER-PM contact site protein Scs2, and NET3C, a member of a plant-specific superfamily of actin-binding proteins, localize to ER-PM contact sites in plant cells, where together they interact with actin and microtubules to help organize these sites [18]. SYTA-GFP localized in a punctate pattern along the plasma membrane that, unlike the dynamic ER network, corresponded to immobile nodes on the cortical ER (Pearson correlation coefficient (PCC) 0.57 ± 0.01, co-occurrence $96.5\% \pm 0.6\%$; Figure 1A, Movie 1). VAP27-GFP, as reported, labeled ER-PM contact sites and the ER tubular network [18]. SYTA-RFP co-localized with VAP27-GFP at the immobile ER-PM contact sites (PCC 0.46 ± 0.01), with $92.0\% \pm 2.4\%$ of SYTA and $85.0\% \pm 3.2\%$ of VAP27 co-occurring at these sites (Figure 1B). Likewise, $94.\% \pm 0.8\%$ of SYTA-GFP and $94.\% \pm 2.\%$ of RFP-tagged Ist2$^{490–946}$, a fragment of yeast Ist2 that localizes to ER-PM contact sites [4], co-localized at these static ER nodes (PCC 0.48 ± 0.01; Figure S1E).

SYTA is required to tether the ER to the plasma membrane

The reticulate architecture of the cortical ER is a consequence of the ER being tethered to the plasma membrane [3, 4]. If SYTA, like E-SYTs and Tcbs, was a ER-PM tethering protein and required to form Arabidopsis ER-PM contact sites, then ER morphology should be abnormal in our Col-0 SYTA knockdown mutant *syta-1* [5] and restored to wild type (wt) morphology when complemented with SYTA. We stably transformed our homozygous *syta-1* mutant with a full-length clone of the endogenous Col-0 *SYTA* genomic locus that included the *SYTA* promoter, and in which the SYTA coding sequence 3'-end was fused to TagRFP-T to produce a tagged functional SYTA-RFP [5]. These rescued lines (*syta-1;gSYTA-RFP*) complemented the inhibition of MP-mediated virus cell-to-cell movement and hypersensitivity to high salt exhibited by *syta-1* [6, 15]: TVCV cell-to-cell spread, assessed as infection site sizes on inoculated leaves, and the rate of root elongation in 100 mM NaCl were restored to the levels in wt Col-0 (Figures S2A–S2D).

To examine ER morphology in wt Col-0, *syta-1* and our *SYTA-RFP* rescued lines, we generated stable mCherry-HDEL transformants and also transiently expressed GFP-HDEL in Arabidopsis leaves [5]. In contrast to the cortical ER reticulate morphology in wt Col-0, the ER in *syta-1* was unstructured, appearing fragmented in stable *syta-1* mCherry-HDEL transformants and collapsed in the interior of *syta-1* cells that transiently expressed GFP-HDEL (Figure 1C and Figures S3A–S3E). High resolution imaging of the latter identified some labeled cortical ER tubules and what may be ER-PM junctions; but, these junctions appeared distorted and did not support the typical ER polygonal structure (Figure S3E), consistent with *syta-1* expressing low levels of a truncated, yet functional form of SYTA [5]. Time-lapse imaging showed rapid ER streaming with no apparent stable nodes in *syta-1*, as opposed to the stable reticulate ER with its static nodes and minimal movements in wt Col-0

(Movies S2 and S3). Importantly, both stable mCherry-HDEL transformants and GFP-HDEL expression showed that normal ER network morphology was restored in *SYTA-RFP* rescued lines (Figure 1C and Figures S3A and S3F–S3I).

We also crossed our *SYTA-RFP* rescued line with a stable Col-0 transformant that expressed YFP-HDEL [17]. Fitting with our VAP27 co-localization studies, SYTA-RFP in these F1 lines localized to static ER-PM junctions that corresponded to stationary nodes on the cortical ER network (co-occurrence 85.% ± 2.0%, PCC 0.38 ± 0.01; Figure 1D). We further identified segregating *YFP-HDEL;syta-1;SYTA-RFP* F2 lines that did not contain the wt *SYTA* locus introduced in the F1 cross (Figure S2E). Endogenous *YFP-HDEL* expression in these F2 lines clearly showed that the fragmented ER in the *syta-1* background (Figure 1C) was restored to its normal reticulate morphology by expression of endogenous SYTA-RFP, which localized to static ER-PM junctions (co-occurrence 86.2 ± 1.5%; PCC 0.32 ± 0.006; Figure 1E). Transient GFP-HDEL expression in *SYTA-RFP* rescued lines gave the same results (Figures S3F–S3I). In both stable and transiently expressing FP-HDEL plants, ~15% of SYTA-RFP appeared on what may be cytoplasmic vesicles (Figures 1D–1E and Figures S3G–3H). As the plant actin cytoskeleton has roles in organizing the ER network and ER-PM contact sites [18, 19], we transiently expressed the filamentous F-actin marker *UtrCH-GFP* [20] in *syta-1* and *SYTA-RFP* rescued lines. The actin cytoskeleton was not altered in either line, nor did SYTA and actin microfilaments co-align in *SYTA-RFP* rescued lines (Figure S2F). Thus, altered microfilaments did not explain the unstructured ER in *syta-1*. We conclude that SYTA at ER-PM contact sites tethers the ER to the plasma membrane in Arabidopsis, as do E-SYTs in mammalian cells and Tcbs in yeast.

SYTA is required for MP^{TVCV} to accumulate in PD

SYTA regulates the cell-to-cell trafficking of MPs encoded by TMV and TVCV, and by *Cabbage leaf curl virus* (CaLCuV, a Begomovirus) and *Turnip mosaic virus* (TuMV, a Potyvirus), and it is necessary for TVCV, CaLCuV and TuMV infectivity in Arabidopsis [5, 6]. SYTA does not regulate secretory traffic [5]. This suggests that SYTA is required for these MPs to target to PD and/or modify PD gating, and raised the question of whether SYTA-tethered ER-PM sites were involved in MP transport to PD. To address this, we focused on MP^{TVCV}. MP^{TMV} and MP^{TVCV} are well characterized models for MP function: both localize to PD throughout infection and, when autonomously expressed, are among the most reliable PD markers [7, 21–23]. We transiently expressed MP^{TVCV}-GFP or PDLP1-GFP in wt Col-0 and *syta-1* leaf cells, and analyzed their accumulation at PD using integrated density measurements. The PD integral membrane protein PDLP1 traffics through the secretory pathway and labels all PD [23, 24]. Thus, PDLP1 assessed protein trafficking to PD via the secretory pathway and was an independent PD marker. At ~24 h post bombardment, MP^{TVCV}-GFP accumulated in PD in *syta-1* to ~50% the levels detected in wt Col-0, whereas we found no statistical difference in PDLP1-GFP accumulation at PD (Figure 2A and Figures S4A–S4D). PD density was the same in both lines: 3.17 ± 0.6 PDLP1-labeled PD per 100 micron cell wall in wt Col-0 vs. 3.19 ± 0.75 in *syta-1*. Thus, SYTA was necessary for MP^{TVCV}, but not for PDLP1, to accumulate in PD and, despite the altered ER morphology, the secretory pathway was not overtly impaired in *syta-1*. This was consistent with our conclusion that SYTA does not regulate secretory traffic [5]. We

expressed secGFP, a secreted form of GFP [25], to further showed this: similar levels of secGFP were secreted in wt Col-0 and *syta-1* (Figures S4E–S4H). Thus, secretory trafficking did not require SYTA activity at ER-PM contact sites, nor was it the route for MP^{TVCV} targeting to PD.

MP^{TVCV} recruits SYTA to PD to form TVCV replication sites

TMV and TVCV replicate their positive-sense RNA genomes at sites that form in association with ER membranes in the cell cortex [7]. Infectious TMV/TVCV replicons that express tagged functional MPs produce infection sites on inoculated leaves that provide a time course of infection and a detailed view of MP^{TMV} and MP^{TVCV} localization throughout infection and in relation to virus replication [7, 21]. Early in infection, MP^{TVCV} and MP^{TMV} are on motile vesicles and associate with cortical ER membranes to form virus replication sites adjacent to PD. These replication sites enlarge and the cortical ER network collapses as infection progresses. At the final stages, MP^{TMV} and MP^{TVCV} are degraded, virus replication sites disappear, and the cortical ER network reappears [7, 21]. SYTA can directly bind MPs *in vitro* [5]. Might MP^{TVCV} interact with SYTA at ER-PM contact sites to form TVCV replication sites adjacent to PD and facilitate viral genome cell-to-cell movement?

To examined this in *N. benthamiana*, we transiently co-expressed SYTA-GFP and MP^{TVCV}-RFP, or expressed SYTA-GFP in leaves inoculated with our TVCV::MP-RFP replicon [7]. As expected, MP^{TVCV} localized to PD in uninfected cells; but, only 33.7 ± 4.4% of SYTA-GFP-labeled ER-PM contact sites were associated with MP^{TVCV}-RFP-labeled PD, and SYTA often appeared to be adjacent to MP^{TVCV} (PCC 0.35 ± 0.02; Figures 3A–3C). Using BiFC, we also did not detect a YFP signal at PD when we co-expressed SYTA-nEYFP and MP^{TVCV}-cEYFP, or SYTA-cEYFP and MP^{TVCV}-nEYFP (Figure S4I). In contrast, early in TVCV infection 76.1 ± 4.0% of SYTA-GFP-labeled ER-PM contact sites were at MP^{TVCV}-RFP-labeled PD, SYTA and MP^{TVCV} co-localized at these PD (PCC 0.44 ± 0.02; Figures 3D–3F), and BiFC analyses of SYTA-nEYFP expressed in TVCV::MP-cEYFP infected cells produced a YFP signal, whereas we did not detect fluorescence when we co-expressed SYTA-nEYFP and free cEYFP, or expressed nEYFP in leaves infected with TVCV::MP-cEYFP (Figures 3G–3I). Using transient expression, BiFC has detected MP^{TMV}-ANK interaction and PDLP1 self-interaction at PD *in planta* [23, 26]. Thus, our findings show that MP^{TVCV} interacted with SYTA early in TVCV infection to recruit SYTA to PD, and suggest that SYTA and MP^{TVCV} did not stably interact in the absence of infection.

At later stages of TVCV infection, ER membrane rearranges to form enlarged cortical viral replication sites in which MP^{TVCV} accumulates [7]. To examine these sites, we infected *syta-1* and *SYTA-RFP* rescued lines with a TVCV::MP-GFP replicon, and also co-expressed SYTA-CFP and RFP-HDEL in *N. benthamiana* leaves infected with TVCV::MP-GFP. To confirm that these replication sites were at PD, and examine whether SYTA or ER were in PD at these sites, we transiently expressed SYTA-CFP and PDLP1-GFP, or GFP-HDEL, in *N. benthamiana* leaves infected with TVCV::MP-RFP. SYTA accumulated and co-localized with MP^{TVCV} and RFP-HDEL within the enlarged viral replication sites adjacent to PD in *N. benthamiana* (SYTA/MP co-occurrence 78. ± 4.0%, PCC 0.61 ± 0.01) (Figure 4), and

with MP^{TVCV} at these sites in infected *SYTA-RFP* rescued lines (Figures 2F–H). In *N. benthamiana*, individual fluorescence intensity measurements showed that MP^{TVCV} and SYTA interacted inside these sites surrounded by ER membrane, which appeared to form a barrier that caged this interaction (Figures 4I–4M). Imaging using PDLP1-GFP showed that SYTA was also present in adjacent PD channels where MP^{TVCV} had moved into a neighboring cell, whereas ER membrane at these sites did not accumulate in PD (Figures 4A–4H). The total number of viral replication sites did not vary among wt Col-0, *syta-1* and *SYTA-RFP* rescued lines; but, these sites were significantly smaller in *syta-1* compared to wt Col-0, and were restored to their normal size in our rescued line, where they accumulated SYTA-RFP (Figures 2B–2E). Our results show that MP^{TVCV} recruits SYTA to PD early in infection, following which SYTA and ER membrane dramatically accumulate and are remodeled to form viral replication sites at PD, where SYTA also accumulates within PD channels that are active in MP^{TVCV} cell-to-cell transport.

SYTA-tethered ER-PM contact sites and virus movement

We show here that Arabidopsis SYTA is essential to form ER-PM contact sites in plant cells, that SYTA at these sites is necessary for MP^{TVCV} to accumulate in PD to promote virus movement, and that MP^{TVCV} interacts with SYTA during infection to recruit and remodel ER-PM contact sites to form viral replication sites adjacent to PD and relocate SYTA within PD active in MP cell-to-cell transport. SYTA has features of both extended and classical SYTs. Like E-Levy, Zheng and Lazarowitz p11 SYTs/Tcbs, SYTA has a predicted SMP domain and is essential for ER-PM tethering to form contact sites. But, E-SYTs/Tcbs are anchored to the ER, and the C2C domain is essential to tether human E-SYTs to the plasma membrane [3, 4]. More like classical SYTs, SYTA has only two C2 domains and localizes to the plasma membrane in plant cells, where it regulates endocytosis and endosome recycling in a C2B-dependent manner, and these features of SYTA are functionally linked with regulating MP activity to alter PD for virus movement [5, 6, 15]. Given the roles of ER-PM contact sites in non-vesicular Ca^{2+} and lipid signaling in mammalian cells and yeast, and of Ca^{2+} in regulating PD gating and virus movement [4, 27–29], our findings suggest a key role for SYTA at ER-PM contact sites in altering PD permeability for virus cell-to-cell movement. We propose that MP^{TVCV}-SYTA interaction disrupts ER-PM contact sites, potentially activating SYTA-mediated membrane fusion to expand and remodel these sites to create TVCV replication sites at PD and position the remodeled sites, and SYTA within the PD channel, to modify Ca^{2+} and/or lipid signaling to alter PD permeability and enable virus cell-to-cell movement, thereby coupling movement with virus replication. The locally perturbed homeostasis might also amplify this process. This model can explain the cortical ER network collapsing during Tobamovirus infection and reforming at late stages when MP^{TVCV} is degraded, viral replication sites disappear and ER-PM contact sites could reform. Coupling of virus replication and movement has been proposed for *Potato virus X* [30], which also creates cortical ER-associated virus replication sites adjacent to PD. However, not all viruses do this, including CaLCuV and TuMV, both of which require SYTA for MP activity at PD [5, 6]. This suggests the significance of MPs interacting with SYTA at ER-PM contact sites is not forming viral replication sites *per se*, but remodeling and recruiting these ER-PM junctions to potentially alter PD permeability.

Experimental Procedures

Supplemental Information includes Supplemental Experimental Procedures, four figures, one table and three movies, and can be found with this article online at:

Supplementary Material

Refer to Web version on PubMed Central for supplementary material.

Acknowledgements

References

1. Chapman ER. How does synaptotagmin trigger neurotransmitter release? Annu. Rev. Biochem. 2008; 77:615–641. [PubMed: 18275379]

2. Moghadam PK, Jackson MB. The functional significance of synaptotagmin diversity in neuroendocrine secretion. Front. Endocrinol. 2013; 4:124.

3. Giordano F, Saheki Y, Idevall-Hagren O, Colombo SF, Pirruccello M, Milosevic I, Gracheva EO, Bagriantsev SN, Borgese N, De Camilli P. PI(4,5)P(2)-dependent and Ca(2+)-regulated ER-PM interactions mediated by the extended synaptotagmins. Cell. 2013; 153:1494–1509. [PubMed: 23791178]

4. Manford AG, Stefan CJ, Yuan HL, Macgurn JA, Emr SD. ER-to-plasma membrane tethering proteins regulate cell signaling and ER morphology. Dev. Cell. 2012; 23:1129–1140. [PubMed: 23237950]

5. Lewis JD, Lazarowitz SG. Arabidopsis synaptotagmin SYTA regulates endocytosis and virus movement protein cell-to-cell transport. Proc. Natl. Acad. Sci. U.S.A. 2010; 107:2491–2496. [PubMed: 20133785]

6. Uchiyama A, Shimada-Beltran H, Levy A, Zheng JY, Javia PA, Lazarowitz SG. The Arabidopsis synaptotagmin SYTA regulates the cell-to-cell movement of diverse plant viruses. Front. Plant Sci. 2014; 5:584. [PubMed: 25414709]

7. Levy A, Zheng JY, Lazarowitz SG. The Tobamovirus *Turnip vein clearing virus* 30-kilodalton movement protein localizes to novel nuclear filaments to enhance virus infection. J. Virol. 2013; 87:6428–6440. [PubMed: 23536678]

8. Schoelz JE, Harries PA, Nelson RS. Intracellular transport of plant viruses: finding the door out of the cell. Mol. Plant. 2011; 4:813–831. [PubMed: 21896501]

9. Craxton M. A manual collection of Syt, Esyt, Rph3a, Rph3al, Doc2, and Dblc2 genes from 46 metazoan genomes--an open access resource for neuroscience and evolutionary biology. BMC Genomics. 2010; 11:37. [PubMed: 20078875]

10. Striegel AR, Biela LM, Evans CS, Wang Z, Delehoy JB, Sutton RB, Chapman ER, Reist NE. Calcium binding by synaptotagmin's C2A domain is an essential element of the electrostatic switch that triggers synchronous synaptic transmission. J. Neurosci. 2012; 32:1253–1260. [PubMed: 22279210]

11. Yao J, Kwon SE, Gaffaney JD, Dunning FM, Chapman ER. Uncoupling the roles of synaptotagmin I during endo- and exocytosis of synaptic vesicles. Nat. Neurosci. 2012; 15:243–249. [PubMed: 22197832]

12. McMahon HT, Kozlov MM, Martens S. Membrane curvature in synaptic vesicle fusion and beyond. Cell. 2010; 140:601–605. [PubMed: 20211126]

13. Min SW, Chang WP, Sudhof TC. E-Syts, a family of membranous Ca2+-sensor proteins with multiple C2 domains. Proc. Natl. Acad. Sci. U.S.A. 2007; 104:3823–3828. [PubMed: 17360437]

14. Toulmay A, Prinz WA. A conserved membrane-binding domain targets proteins to organelle contact sites. J. Cell Sci. 2012; 125:49–58. [PubMed: 22250200]

15. Schapire AL, Voigt B, Jasik J, Rosado A, Lopez-Cobollo R, Menzel D, Salinas J, Mancuso S, Valpuesta V, Baluska F, et al. Arabidopsis Synaptotagmin 1 Is required for the maintenance of plasma membrane integrity and cell viability. Plant Cell. 2008; 20:3374–3388. [PubMed: 19088329]

16. Schauder CM, Wu X, Saheki Y, Narayanaswamy P, Torta F, Wenk MR, De Camilli P, Reinisch KM. Structure of a lipid-bound extended synaptotagmin indicates a role in lipid transfer. Nature. 2014; 510:552–555. [PubMed: 24847877]

17. Nelson BK, Cai X, Nebenfuhr A. A multicolored set of in vivo organelle markers for co-localization studies in Arabidopsis and other plants. Plant J. 2007; 51:1126–1136. [PubMed: 17666025]

18. Wang P, Hawkins TJ, Richardson C, Cummins I, Deeks MJ, Sparkes I, Hawes C, Hussey PJ. The plant cytoskeleton, NET3C, and VAP27 mediate the link between the plasma membrane and endoplasmic reticulum. Curr. Biol. 2014; 24:1397–1405. [PubMed: 24909329]

19. Boevink P, Oparka K, Santa Cruz S, Martin B, Betteridge A, Hawes C. Stacks on tracks: the plant Golgi apparatus traffics on an actin/ER network. Plant J. 1998; 15:441–447. [PubMed: 9750355]

20. Burkel BM, von Dassow G, Bement WM. Versatile fluorescent probes for actin filaments based on the actin-binding domain of Utrophin. Cell Motil. Cytoskeleton. 2007; 64:822–832. [PubMed: 17685442]

21. Heinlein M, Padgett HS, Gens JS, Pickard BG, Casper SJ, Epel BL, Beachy RN. Changing patterns of localization of the *Tobacco mosaic virus* movement protein and replicase to the endoplasmic reticulum and microtubules during infection. Plant Cell. 1998; 10:1107–1120. [PubMed: 9668131]

22. Sagi G, Katz A, Guenoune-Gelbart D, Epel BL. Class 1 reversibly glycosylated polypeptides are plasmodesmal-associated proteins delivered to plasmodesmata via the Golgi apparatus. Plant Cell. 2005; 17:1788–1800. [PubMed: 15879561]

23. Thomas CL, Bayer EM, Ritzenthaler C, Fernandez-Calvino L, Maule AJ. Specific targeting of a plasmodesmal protein affecting cell-to-cell communication. PLoS Biology. 2008; 6:e7. [PubMed: 18215111]

24. Bayer E, Thomas CL, Maule AJ. Symplastic domains in the Arabidopsis shoot apical meristem correlate with PDLP1 expression patterns. Plant Signal. Behav. 2008; 3:853–855. [PubMed: 19704520]

25. Batoko H, Zheng HQ, Hawes C, Moore I. A Rab1 GTPase is required for transport between the endoplasmic reticulum and Golgi apparatus and for normal Golgi movement in plants. Plant Cell. 2000; 12:2201–2217. [PubMed: 11090219]

26. Ueki S, Spektor R, Natale DM, Citovsky V. ANK, a host cytoplasmic receptor for the *Tobacco mosaic virus* cell-to-cell movement protein, facilitates intercellular transport through plasmodesmata. PLoS Pathogens. 2010; 6:e1001201. [PubMed: 21124937]

27. Chang CL, Hsieh TS, Yang TT, Rothberg KG, Azizoglu DB, Volk E, Liao JC, Liou J. Feedback regulation of receptor-induced Ca^{2+} signaling mediated by E-Syt1 and Nir2 at endoplasmic reticulum-plasma membrane junctions. Cell Rep. 2013; 5:813–825. [PubMed: 24183667]

28. Roberts AG, Oparka KJ. Plasmodesmata and the control of symplastic transport. Plant Cell Environ. 2003; 26:103–124.

29. Zavaliev R, Ueki S, Epel BL, Citovsky V. Biology of callose (beta-1,3-glucan) turnover at plasmodesmata. Protoplasma. 2011; 248:117–130. [PubMed: 21116665]

30. Tilsner J, Linnik O, Louveaux M, Roberts IM, Chapman SN, Oparka KJ. Replication and trafficking of a plant virus are coupled at the entrances of plasmodesmata. J. Cell Biol. 2013; 201:981–995. [PubMed: 23798728]

Highlights

- SYTA is essential to form ER-plasma membrane (ER-PM) contact sites in Arabidopsis

- MP^{TVCV} recruits SYTA to plasmodesmata for virus replication and movement

- Tobamovirus replication sites contain MP^{TVCV}-SYTA complexes caged by ER membrane

- SYTA at ER-PM contact sites is required for MP^{TVCV} to accumulate in plasmodesmata
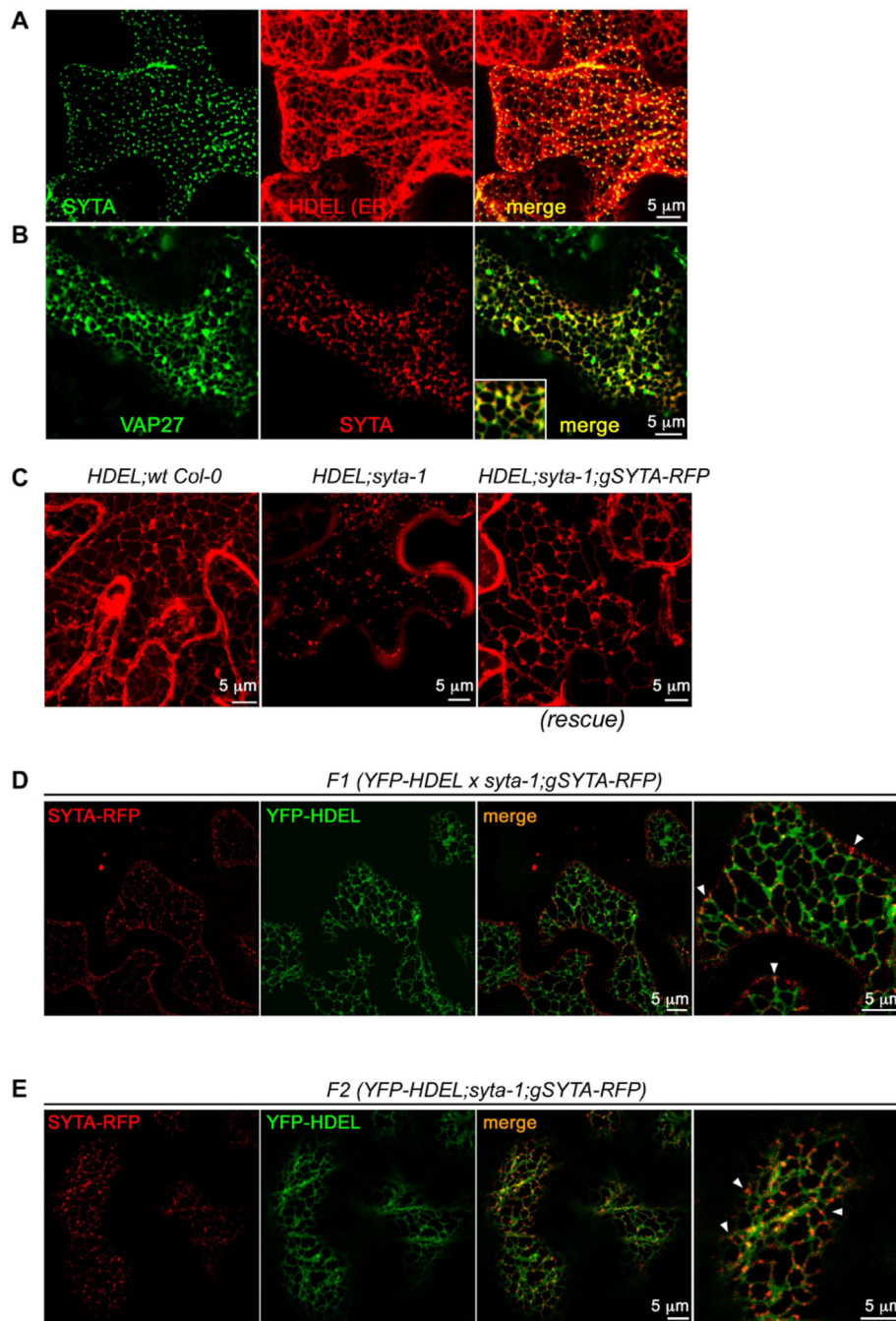
Figure 1. SYTA localizes to, and is required to form, ER-PM contact sites

(A) Confocal images of SYTA-GFP and RFP-HDEL expressed in *N. benthamiana* leaf epidermal cells show SYTA localized to immobile cortical ER nodes (co-occurrence 96.5% ± 0.6%, PCC 0.57 ± 0.01).

(B) Confocal images of SYTA-RFP and Arabidopsis VAP27-GFP expressed in *N. benthamiana* leaf epidermal cells show SYTA localized to VAP27-labeled ER-PM contact sites (co-occurrence 92.0% ± 2.4% for SYTA and 85.0% ± 3.2% for VAP27, PCC 0.46 ± 0.01).

(C–E) Confocal images of ER markers mCherry-HDEL or YFP-HDEL endogenously expressed in stable Arabidopsis Col-0 wt, *syta-1* mutant or *SYTA-RFP* rescued (*syta-1;gSYTA-RFP*) lines. Images in (C) are projected Z series. Far right panels in (D) and (E) show enlargements of a region in each adjacent merged panel to highlight localization of SYTA-RFP at ER-PM junctions (arrowheads mark a few examples).

(C) Stable transformants expressing mCherry-HDEL show (left) normal ER morphology in wt Col-0, (middle) fragmented appearance of the ER in *syta-1*, and (right) restoration of normal ER network morphology in *SYTA-RFP* rescued line (*syta-1;gSYTA-RFP*).

(D) Stable outcrossed *YFP-HDEL x syta-1;gSYTA-RFP* F1 line shows SYTA-RFP localized to stationary nodes on the cortical ER network at the plasma membrane (ER-PM junctions; co-occurrence 85. ± 2.0%, PCC 0.38 ± 0.01).

(E) Stable *YFP-HDEL;syta-1;gSYTA-RFP* F2 segregant line homozygous for SAIL 775 A08 (*syta-1*) T-DNA insertion [5] at the *SYTA* locus shows ER restored to normal reticulate morphology by expression of endogenous SYTA-RFP, which localized to stationary cortical ER nodes at the plasma membrane (co-occurrence 86.2 ± 1.5%, PCC 0.32 ± 0.006) in this *SYTA-RFP* rescued line.

Scale bars as indicated. See also Figures S1, S2 and S3, and Movies S1, S2 and S3.
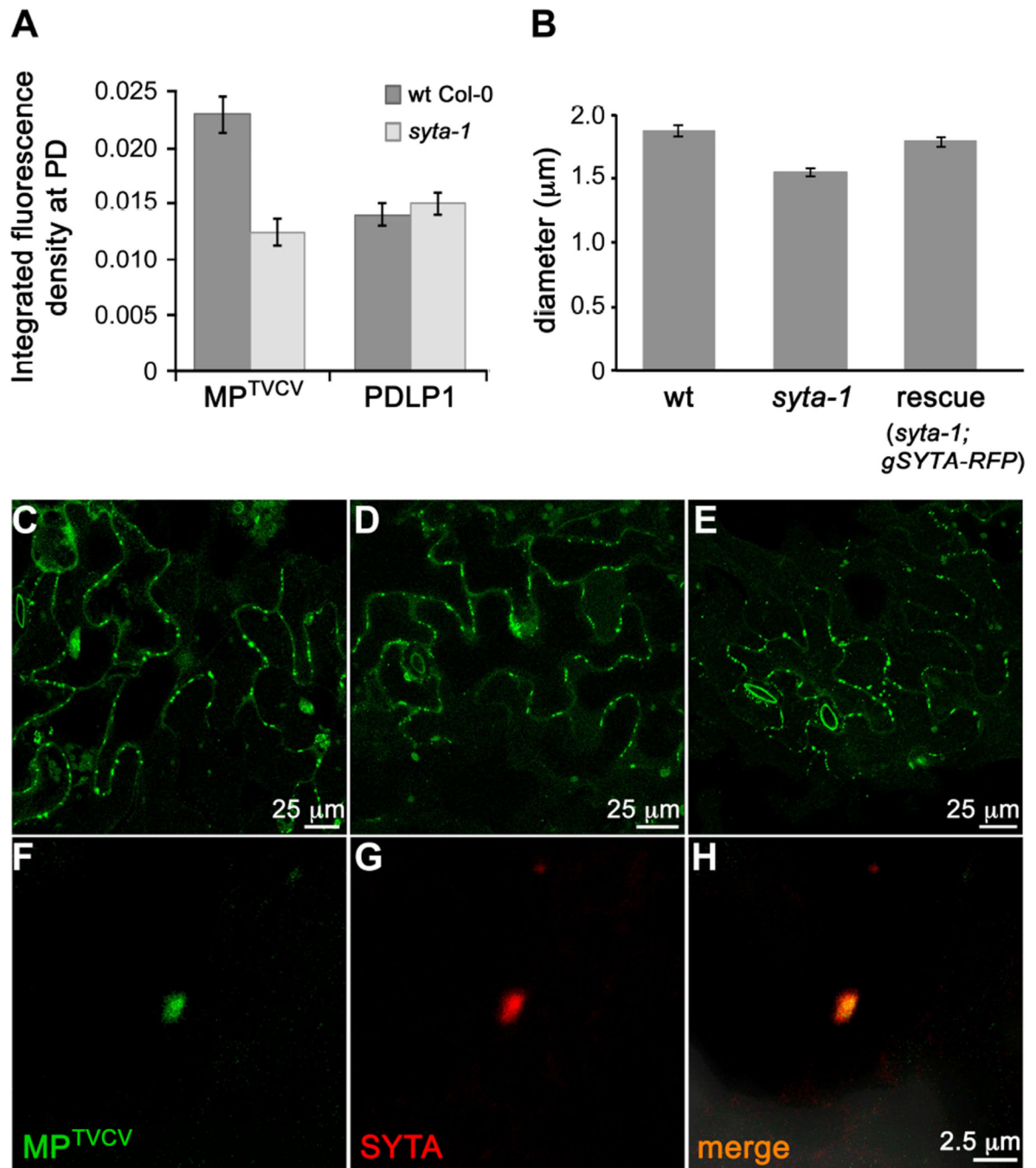
Figure 2. Endogenous SYTA is required for MP^{TVCV} to traffic to PD and co-localizes with MP^{TVCV} in virus replication sites at PD in Arabidopsis

(A) Accumulation of MP^{TVCV}-GFP and PDLP1-GFP at PD in leaf epidermal cells of wt and *syta-1* plants. Data are mean ± SE. *t*-test P<0.0001 for MP^{TVCV} and P>0.5 for PDLP1 at PD in wt vs. *syta-1*.

(B) Sizes (diameter) of TVCV replication sites in TVCV::MP-GFP replicon infected wt Col-0, *syta-1* or *SYTA-RFP* rescued line. A total of 380, 430 and 342 replication sites were measured in wt Col-0, *syta-1* and the *SYTA-RFP* rescued line, respectively (ANOVA and Tukey's HSD P<0.0001).

(C–E) Confocal images of MP^{TVCV}-GFP labeled virus replication sites at late stages in (C) wt Col-0, (D) *syta-1* and (E) *SYTA-RFP* rescued line (*syta-1;gSYTA-RFP*) infected with TVCV::MP-GFP replicon.

(F–H) Confocal images of endogenous SYTA-RFP at late stages in a replicon TVCV::MP-GFP infected cell in Arabidopsis *SYTA-RFP* rescued line show SYTA and MP^{TVCV} co-localizing in a TVCV cortical replication site.

Scale bars as indicated. See also Figure S4.
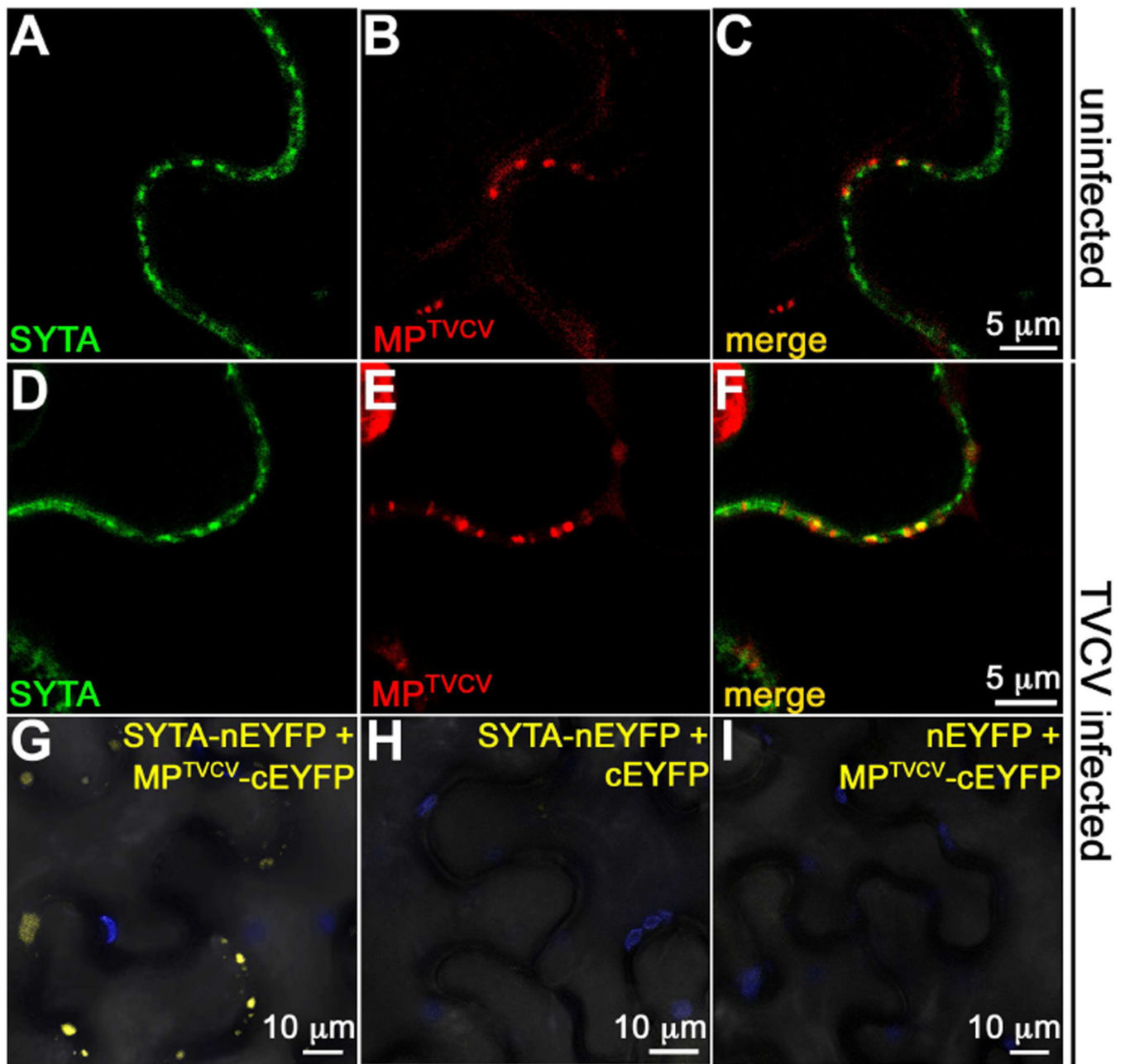
Figure 3. MP^{TVCV} and SYTA interact in TVCV-infected cells

(A–C) Confocal images of SYTA-GFP and MP^{TVCV}-RFP co-expressed in uninfected *N. benthamiana* leaf epidermal cells show SYTA at ER-PM junctions that appear to be adjacent to MP^{TVCV} in PD (co-occurrence $33.7 \pm 4.4\%$, PCC 0.35 ± 0.02).

(D–F) Confocal images of SYTA-GFP and MP^{TVCV}-RFP expressed early in infection (leading edge) in TVCV::MP-RFP infection sites on *N. benthamiana* leaves. Transiently expressed SYTA and MP^{TVCV} expressed from the TVCV replicon co-localize in early cortical ER-associated virus replication sites formed at PD (co-occurrence $76.1 \pm 4.0\%$, PCC 0.44 ± 0.02).

(G–I) BiFC of SYTA-nEYFP expressed in TVCV::MP-cEYFP infection site in *N. benthamiana* show SYTA-MP^{TVCV} interaction (YFP fluorescence) within cortical virus replication sites. No signal was detected when SYTA-nEYFP and cEYFP were co-expressed, or nEYFP was expressed in TVCV::MP-cEYFP infected cells. Blue is chloroplast autofluorescence.

Scale bars as indicated. See also Figure S4.
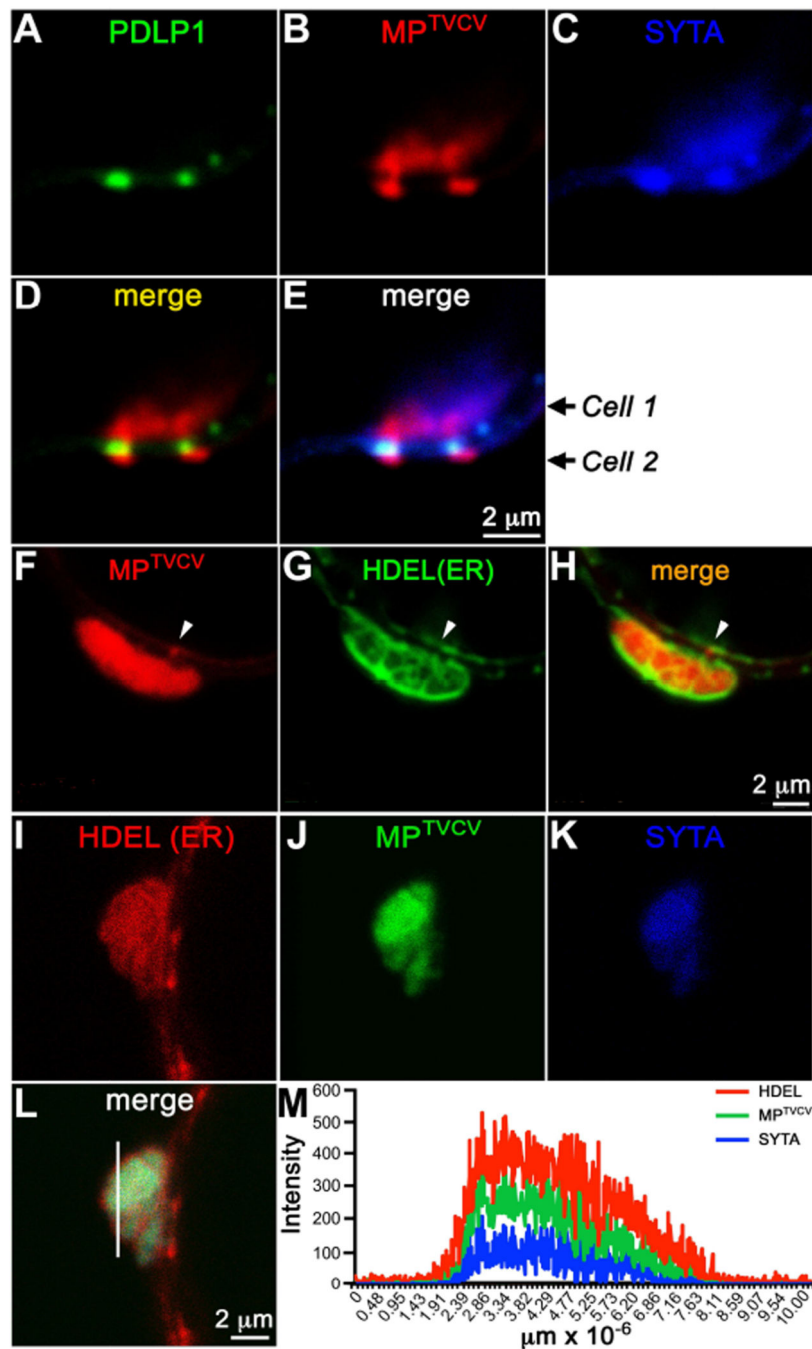
Figure 4. SYTA and MP^TVCV co-localize in virus replication sites at PD in *N. benthamiana*
(A–E) Confocal images of SYTA-CFP and PDLP1-GFP (PD marker) at late stages in a replicon TVCV::MP-RFP infected cell (Cell 1) in *N. benthamiana* show (A–C, E) SYTA and MP^TVCV co-localizing in virus replication sites formed in the cell cortex adjacent to two PD, and (C, E) SYTA also accumulating within the PD, while (B, D) MP^TVCV has moved into a neighboring cell (Cell 2).

(F–H) Confocal images of GFP-HDEL at late stages in a replicon TVCV::MP-RFP infected cell in *N. benthamiana* show MP^TVCV accumulating in ER membrane-containing (HDEL

marker) replication sites formed in the cell cortex adjacent to PD. MP^{TVCV}, but not HDEL (ER), can also be seen within PD at some sites (arrow).

(I–L) Confocal images of SYTA-CFP and RFP-HDEL at late stages in a replicon TVCV::MP-GFP infected cell in *N. benthamiana* show SYTA, MP^{TVCV} and HDEL (ER marker) co-localizing within a TVCV cortical replication site.

(M) Fluorescence intensities of SYTA-CFP, MP^{TVCV}-GFP and RFP-HDEL across a section in the replication site (line in L) show MP^{TVCV} and SYTA within the site caged by ER membrane.

Scale bars as indicated.